Biomaterials 33 (2012) 2282–2288

Contents lists available at SciVerse ScienceDirect

Biomaterials

journal homepage: www.elsevier.com/locate/biomaterials

A pyrene-imidazolium derivative that selectively Recognizes G-Quadruplex DNA

Ha Na Kim [a,1], Eun-Hae Lee [b,1], Zhaochao Xu [a,c,1], Hee-Eun Kim [b], Hee-Seung Lee [d], Joon-Hwa Lee [b,**], Juyoung Yoon [a,e,*]

[a] Department of Chemistry and Nano Science, Ewha Womans University, Seoul 120-750, Republic of Korea
[b] Department of Chemistry and RINS, Gyeongsang National University, Jinju, Gyeongnam 660-701, Republic of Korea
[c] Dalian Institute of Chemical Physics, Chinese Academy of Sciences, Dalian 116023, China
[d] Molecular-Level Interface Research Center, Department of Chemistry, KAIST, Daejeon 305-701, Republic of Korea
[e] Department of Bioinspired Science, Ewha Womans University, Seoul 120-750, Republic of Korea

ARTICLE INFO

Article history:
Received 11 October 2011
Accepted 25 November 2011
Available online 21 December 2011

Keywords:
G-quadruplex
NMR
Fluorescent sensor
Imidazolium
Pyrene
Excimer emission

ABSTRACT

G-quadruplexes, formed of four stranded guanine bases stabilized by monovalent cations, serve important role in cancer cell growth and control gene expression in telomere. Since there are various types of quadruplex structures, rapid and simple screening methods with high selectivity, sensitivity and nontoxicity are required for understanding about the biological roles of quadruplex DNA as well as in designing therapeutics. Herein, we report a pyrene-imidazolium derivative, **JY-1**, which can with high selectivity recognize G-quadruplex using fluorescence and NMR spectroscopy. This is the first example based on the imidazolium derivative, which can detect the G-quadruplex directly to utilize the excimer/monomer emission change in pyrene fluorophore. The selectivity of strong binding to a specific sequence can allow for quadruplex sensing and the detection method presented here is very simple, using fluorescence and NMR study. Also, the groove binding characteristic of **JY-1** to the G-quadruplex has a relatively low nonspecific toxicity and the structure-specific differences in fluorescent character between DNA duplex and G-quadruplex may offer more discovery and application in biological study.

1. Introduction

For many years, the development of DNA sensing and recognition technology has attracted a great deal of attention since various diseases and genetic disorders have been found to be directly related to changes in DNA [1–4]. Among the various types of secondary structures in human DNA, such as B-DNA, Z-DNA, hair pins, *etc* [5]., guanine rich sequences like, G-quadruplexes serve an important role in cancer cell growth and control gene expression in telomeres [6]. G-quadruplexes are composed of four stranded guanine bases stabilized by monovalent cations such as Na^+ or K^+ between tetrad guanine bases [7]. Recent studies show that this unique structure can be formed not only in the telomeric region of the genome, but also among other guanine rich sequences having the potential to form quadruplex elsewhere in the human genome [8,9]. Efficient detection of G-quadruplex in addition to stabilization of the G-quadruplex structure is very helpful in designing cancer drugs and in diagnosis of various diseases [10,11]. Detection method taking advantage of fluorescence is so much simple and sensitive [12–15] that there have been reports on fluorophore labelled G-quadruplex oligonucleotide [16–18] or label free probe systems for sensing G-quardruplex [19–23]. However, these studies mainly set out to probe potassium ion stabilizing in G-quartet structure, or detect the conformational change of the G-quartet. Some studies were performed using a labelled oligonucleotide system, which is expensive and laborious. In addition, the intercalative methods for detection of the quadruplex can be cytotoxic with relatively low selectivity and can induce the destabilization of the quadruplex within telomeres, which is critical for telomerase activity inhibition [6]. Since there are various types of quadruplex structures, rapid and simple screening methods with high selectivity, sensitivity and nontoxicity are required for understanding the biological roles of quadruplex DNA as well as for designing therapeutics [24,25].

Herein, we report a pyrene-imidazolium derivative which can with high selectivity recognize G-quadruplex. Imidazolium based receptors have been investigated for the reconition of various anionic species [26–35]. We have synthesized a quadruplex selective fluorescent probe, **JY-1** (Fig. 1A), designed on the structural combination of a highly effective binding with DNA by using

* Corresponding author. Fax: +82 2 3277 2384.
** Corresponding author. Department of Chemistry and RINS, Gyeongsang National University, Jinju, Gyeongnam 660-701, Republic of Korea. Fax: +82 55 772 1489.
E-mail addresses: joonhwa@gnu.ac.kr (J.-H. Lee), jyoon@ewha.ac.kr (J. Yoon).
[1] contributed equally to this work.

0142-9612/$ – see front matter © 2011 Elsevier Ltd. All rights reserved.
doi:10.1016/j.biomaterials.2011.11.073

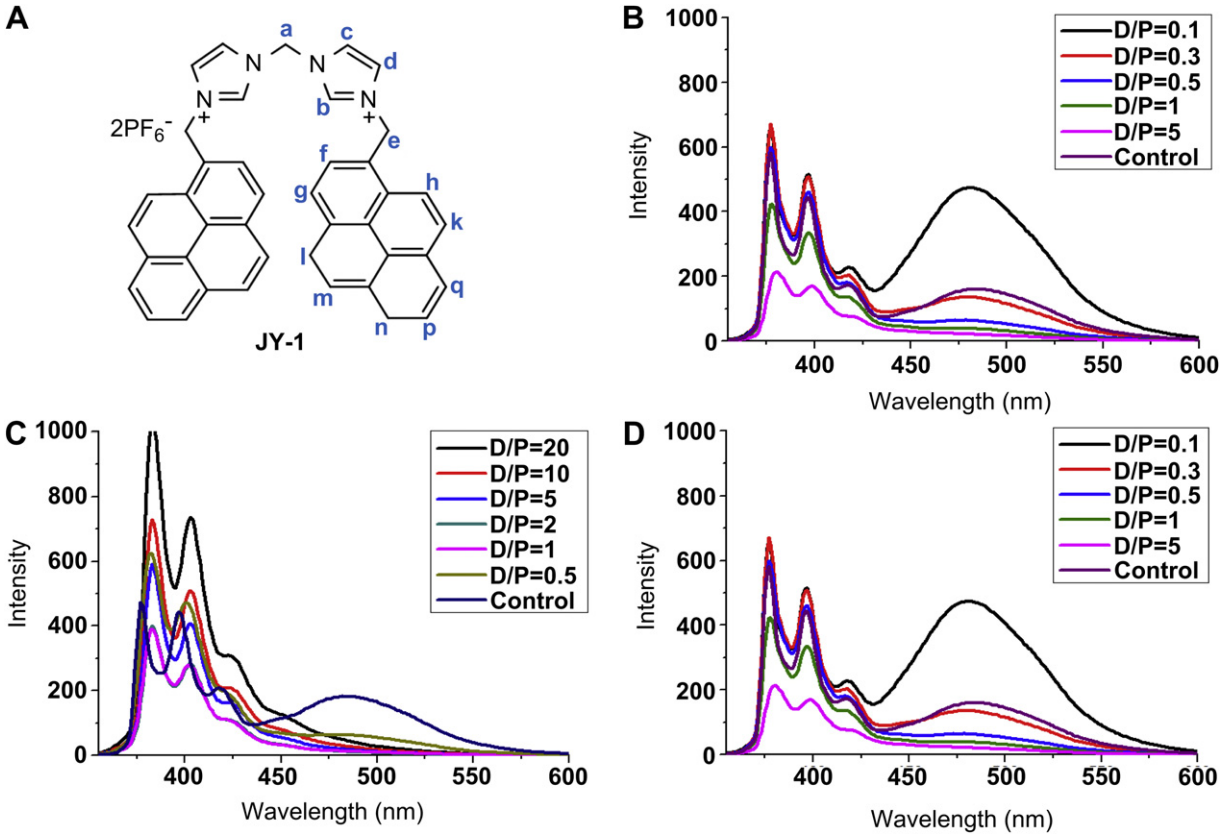

Fig. 1. (a) Chemical structure of pyrene derivatives, **JY-1**. (b–c) Fluorescence emission spectra of **JY-1** complexed with (b) DNA-1 or (c) DNA-2 duplexes in the aqueous solution containing 10 mM sodium phosphate (pH = 7.0) at various D/P ratios. (d) Fluorescence emission spectra of **JY-1** complexed with DNA-3 (D/*P* = 1.0) in the aqueous solution containing 10 mM HEPES buffer (pH = 7.4) with various KCl concentrations. (Control : **JY-1** only, D: DNA, P: **JY-1**).

imidazolium unit, and inducing distinctive fluorescent emission changes. In order to account for the selective recognition of the **JY-1** to G-quartet DNA, we have performed NMR and fluorecence study on the **JY-1** complexed with various DNA molecules (*see* Table 1).

2. Materials and methods

2.1. Synthesis

Compound **2**:The suspension of 1-pyrenemethanol **4** (2 g, 8.6 mmol) in toluene (100 mL) was cooled to 0 °C followed by addition of phosphorus tribromide (1 mL, 10.5 mmol) via syringe. The mixture was stirred at 0 °C for 1 h and then warmed to room temperature, during which the reaction became homogeneous. Saturated Na_2CO_3 solution 50 mL was added slowly and the reaction was stirred until it cooled to room temperature. The phases were separated, and the organic phase was washed with H_2O (50 mL × 2), brine (50 mL × 2) and dried over Mg_2SO_4. The yellow filtrate was concentrated to minium volume. The yellow needle-like solid was collected and dried. The mother liquid was concentrated again and repeated the crystallization process. The total product was 2.3 g in 91% yield. m.p. = 136 °C ^{1}H-NMR ($CDCl_3$, 250 MHz) δ 5.23 (s, 2H), 8.02 (m, 5H), 8.21 (m, 3H), 8.35 (d, *J* = 9.3 Hz, 1H). ^{13}C-NMR ($CDCl_3$, 62.5 MHz) δ 32.28, 122.80, 124.58, 124.84, 125.07, 125.61, 126.26, 127.32, 127.67, 128.01, 128.22, 129.03, 130.51, 130.73, 131.17, 131.92.

Compound **JY-1**:A solution of 1-bromomethylpyrene **2** (0.66 g, 2.24 mmol) and bisimidazole **3** (0.15 g, 1 mmol) in 160 mL acetonitrile was refluxed for 24 h under argon. After cooling to the room temperature, the precipitate was filtered and washed with ether. The bromide salt (694 mg, 93%) was dissolved in 25 mL DMF. (During the dropwise addition of saturated aqueous KPF_6 solution, precipitate was formed. After washing the precipitate several times with water, desired product was obtained as a white solid (663 mg, 81%). ^{1}H-NMR (DMSO, 250 MHz) (for bromide salt) δ 6.31 (s, 4H), 6.58 (s, 2H), 8.02 (s, 2H), 8.03 (s, 2H), 8.08–8.52 (m, 18 H), 9.51 (s, 2H). ^{13}C-NMR (DMSO, 62.5 MHz) δ 50.39, 58.29, 122.36, 123.53, 123.56, 124.04, 125.17, 125.83, 125.93, 126.06, 126.54, 126.71, 127.19, 128.29, 128.72, 128.84, 130.06, 130.61, 131.61, 137.62.; HRMS (FAB) calcd for $C_{41}H_{30}F_6N_4P$ $[M\text{-}PF_6]^+$ 723.2101, found 723.2111.

2.2. Fluorescence study

Oligonucleotides were purchased from Bioneer(South Korea) and dissolved in 10 mM phosphate buffer, containing 100 mM NaCl, 0.1 mM EDTA, pH 7.0. This buffer solution was used during the whole fluorescent experiments except for DNA-3 study with KCl. The compound (1 mM) stock in CH_3CN was prepared and the final test samples were made up in 1% CH_3CN and 99% buffer solution. For all measurements, excitation was at 343 nm. Both excitation and emission slit widths were 3 nm or 5 nm. Fluorescence emission spectra were obtained using RF-5301/PC Spectrofluorophotometer (Shimadzu).

2.3. Circular dichroism (CD) measurement

The CD spectra were recorded on a JASCO J-810 spectropolarimeter. Solutions containing the probe and oligonucleotides were placed in a quartz cell (1 cm path length), and the spectra were recorded in the 190–450 nm region.The parameters of measurement were 1 nm bandwidth, standard sensitivity and response time of 4 s. Each sample was scanned 3 times and the averages were obtained. The baseline was corrected from the buffer solution containing 1% CH_3CN.

Table 1
Sequence contexts of DNA studied here([a]: Single-stranded DNA).

Name	Sequence	Type
DNA-1	d(ACCCACCCAA)/d(TTGGGTGGGT)	duplex
AC-10	d(ACCCACCCAA)	ssDNA[a]
TG-10	d(TTGGGTGGGT)	ssDNA
DNA-2	d(GTCATGGTTA)/d(TAACCATAGC)	duplex
DNA-3	d(GGTTGGTGTGGTTGG)	G-quartet
GGG	d(GGG)	ssDNA trimer
TGG	d(TGG)	ssDNA trimer
GTG	d(GTG)	ssDNA trimer
GGT	d(GGT)	ssDNA trimer
TTG	d(TTG)	ssDNA trimer

2.4. NMR experiment

All DNA and **JY-1** samples were dissolved in 60% H_2O/10% D_2O/30% CD_3CN buffer containing 5 mM sodium phosphate (pH 8.0) and 50 mM NaCl. All NMR experiments were performed on a Varian Inova 600 MHz spectrometer (KAIST, Daejeon) using a HCN triple-resonance probe. One dimensional (1D) NMR data were processed with either the program VNMR J (Varian, Palo Alto) or FELIX2004 (Accelrys, San Diego), whereas 2D data were processed with the program NMRPIPE and analyzed with the program Sparky.

3. Results and discussion

3.1. Design, synthesis, and fluorescence study of compound *JY-1*

For the synthesis of **JY-1** (Fig. 1A), 1-bromomethylpyrene (**2**) was prepared by treating 1-pyrenemethanol (**4**) with phosphorous tribromide in toluene (*see* Scheme 1). 1-bromomethylpyrene was then reacted with bisimidazole (**3**) followed by anion-exchange with KPF_6, yielding 81% **JY-1** (*see* Scheme 1). Fig. 1 shows the fluorescence emission spectra of **JY-1** with various DNA in aqueous solution. In the absence of DNA, **JY-1** shows the distinctive spectra with the monomer emission and excimer emission at 375 and 482 nm, respectively. There were no significant changes in the emission spectra of **JY-1** when 10 equivalents of various phosphate and nucleotide anions were added (Supporting information S-Figure 1). Surprisingly, **JY-1** displayed fluorescent enhancement of the excimer peak (482 nm) upon the addition of DNA-1 duplex even at the DNA/**JY-1** molar ratio (D/P ratio) = 0.1 in 10 mM sodium phosphate buffer (Fig. 1B). However, when DNA-2, random DNA decamer duplex, was added, no significant enhancement of the excimer fluorescence peak at 482 nm was observed even with the D/P ratio of 20 (Fig. 1C). On the other hand, the intensity of monomer peak increased upon interaction with DNA-2, as the D/P ratio increased (Fig. 1C). These data indicate that **JY-1** binds with DNA-1 through unusual molecular interaction unlike DNA-2.

3.2. NMR studies for prove the interaction between *JY-1* and DNA complexes

To understand this unusual interaction, we performed ^{1}H-NMR experiments on the **JY-1**/DNA-1 complex. The assignment for the proton resonances of the **JY-1** were made by the analysis of NOESY spectra at 25 °C (see Fig. 2). Fig. 2A shows the titration of the DNA-1 duplex with **JY-1**, where the imino proton resonances extensively broadened as **JY-1** was added and then completely disappeared at the D/P ratio = 1.0. ^{1}H-NMR spectra of **JY-1** were also dramatically changed by addition of the DNA-1 duplex, indicating specific interaction between DNA-1 and **JY-1** (Fig. 2B). These results clearly demonstrated that the double helix of DNA-1 was destabilized upon interaction with **JY-1** and subsequently melted out to single strands. To further clarify this interaction, the titrations of **JY-1** with each strand of DNA-1 (TG-10 and AC-10) were monitored by 1D NMR spectra (Fig. 2C and D). Interestingly, like DNA-1, the TG-10 strand caused a significant change in the NMR spectra of **JY-1** (Fig. 2B). Even though the D/P ratio is only 0.1, the NMR spectra of these complexes were completely different from that of free **JY-1** (Fig. 2D). For example, at D/*P* = 0.1, the peaks a and e are disappeared upon binding to the TG-10 strand and new four resonances observed at that region (Fig. 2C). In the free **JY-1**, each methylene moiety which connect between two imidazolium rings (peak a) or between imidazolium and pyren rings (peak e) shows only one signal in the proton NMR spectrum. However, in the case of the **JY-1**/TG-10 complex, the methylene protons positioned at a and e exhibit more than two resonances because the pyren and imidazolium rings cannot rotate freely any more. In the case of AC-10, no clear change in the NMR spectra of **JY-1** was observed, as the D/P ratio increased up to 1.0 (Fig. 2D). The slight upfield shifts of some resonances of **JY-1**, such as a resonance at 6.3 ppm (peak e), imply a nonspecific interaction between the imidazolium cation of **JY-1** and the phosphate anion of AC-10 (Fig. 2C). From these results, the molecular interaction between **JY-1** and DNA-1 duplex can be summarized as follows: *i*) **JY-1** destabilizes the double helix of DNA-1 and then separates it into two single strands, TG-10 and AC-10; *ii*) **JY-1** selectively binds to the single-stranded TG-10 and exhibits a unique conformation in the complex; *iii*) **JY-1** in this unique conformation can emit the excimer fluorescence.

3.3. NMR study of compound *JY-1* for selective GGG trimer detection

The single-stranded TG-10 has a G-rich sequence and can form G-quartet DNA helix under KCl buffer conditions. To address the correlation between the G-quartet DNA structure and the excimer fluorescence of **JY-1**, the fluorescence study on the TG-rich 15mer, DNA-3, which is known as a thrombin-binding aptamer and can form the G-quartet structure with K^+ ion [12], was performed. Here, the HEPES buffer (pH 7.4) was used instead of 10 mM sodium phosphate buffer containing 100 mM NaCl to exclude the Na^+ ion effect because some metal cations including K^+, Na^+, or Pb^{2+} can stabilize the G-quartet structure [36,37]. Surprisingly, **JY-1** showed significant excimer fluorescence as the KCl concentration increased (Fig. 1D). From these results, we can suggest the hypothesis that the excimer fluorescence is a unique characteristic of **JY-1** complexed with G-quartet DNA.

In order to verify this hypothesis, we performed the fluorescence and NMR experiments on the **JY-1** complexed with five DNA trimers (TTG, TGG, GGG, GGT, and GTG), which are designed from cutting the TG-10 into trimers and GG dimer (Fig. 3). This approach provides the information for the minimum sequence requirement for DNA binding of the **JY-1** molecule. Only GGG trimer induced the large enhancement of excimer emission from **JY-1**, whereas other trimers and GG dimer did not induce the excimer emission (Fig. 3A). These results indicate that there is a unique interaction between **JY-1** and GGG trimer sequence. To prove the interaction, the NMR study of **JY-1** with GGG and TTG trimers was also performed and then compared with each other (Fig. 3C and D). Fig. 3C shows the titration of the GGG trimer to **JY-1** dissolved in the NMR

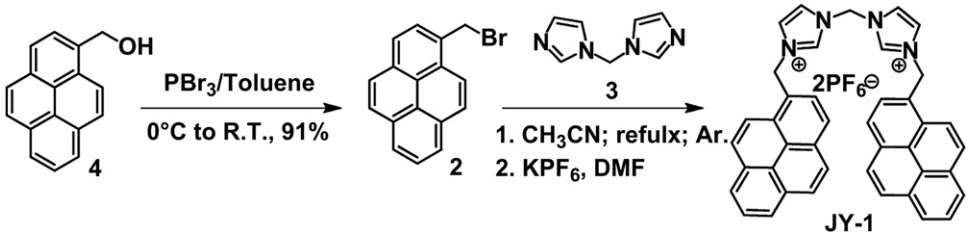

Scheme 1. Synthesis of **JY-1**.

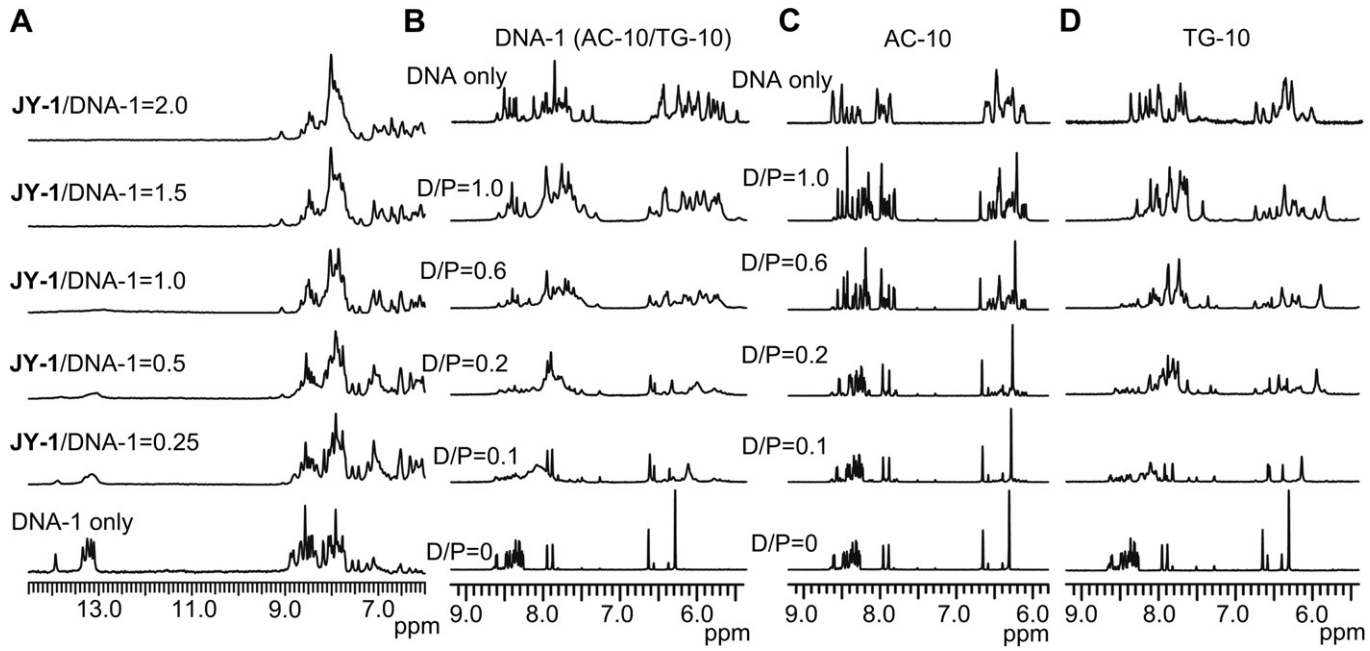

Fig. 2. (A) 1D ^{1}H-NMR spectra of free DNA-1 (top) and DNA-1–**JY-1** complexes in 60% H_2O/10% D_2O/30% CD_3CN buffer containing 5 mM sodium phosphate (pH 8.0) and 50 mM NaCl at 25 °C. The **JY-1**/DNA-1 ratios (inverse D/P ratios) are shown on the left of each spectrum. 1D ^{1}H-NMR spectra of **JY-1** in 70% D_2O/30% CD_3CN buffer containing 5 mM sodium phosphate (pH 8.0) and 50 mM NaCl at 25 °C upon titration with (B) DNA-1 duplex, (C) TG-10, or (D) TG-10. 1D ^{1}H-NMR spectra of free DNA-1, TG-10 and AC-10 are shown on the top of the spectra.

buffer (60% H_2O/10% D_2O/30% CD_3CN, 5 mM sodium phosphate (pH = 8.0) and 50 mM NaCl). Like TG-10, at D/*P* = 1.5, the peaks a and e are disappeared upon binding to the GGG trimer and new resonances are observed at that region (Fig. 3C). This data indicates that the **JY-1** binds to the GGG trimer with similar binding mode to TG-10 strand. Thus, NMR structural study of the **JY-1**/GGG complex can provide structural information about the general interaction between **JY-1** and G-rich DNA strand. Surprisingly, six sharp peaks at 10–11.5 ppm, corresponding to guanine imino protons of G-quartet structure, appeared as the amount of GGG increased (Fig. 3C). Under this condition, free GGG showed no imino proton resonances (Fig. 3B). These results indicate that, under our experimental condition, free GGG did not form G-quartet structure but **JY-1** interacts with unstructured GGG and induces the G-quartet structure of the GGG trimer, which shows some imino resonances at 10–11.5 ppm. When TTG was added to **JY-1**, this type of imino proton resonance was not observed, indicating that **JY-1** could not induce the G-quartet structure in the case of the TTG trimer (Fig. 3D).

3.4. Structural binding model studies

In order to indentify the suitable geometry of the induced G-quatet structure, the NOESY experiments on the **JY-1**–GGG complex were performed. Six imino peaks of this complex indicate that four molecules of GGG form two-fold symmetric G-quartet structure. The non-exchangeable base (H8) and sugar (H1′, H2′, H2″) protons of GGG in the complex were assigned according to their

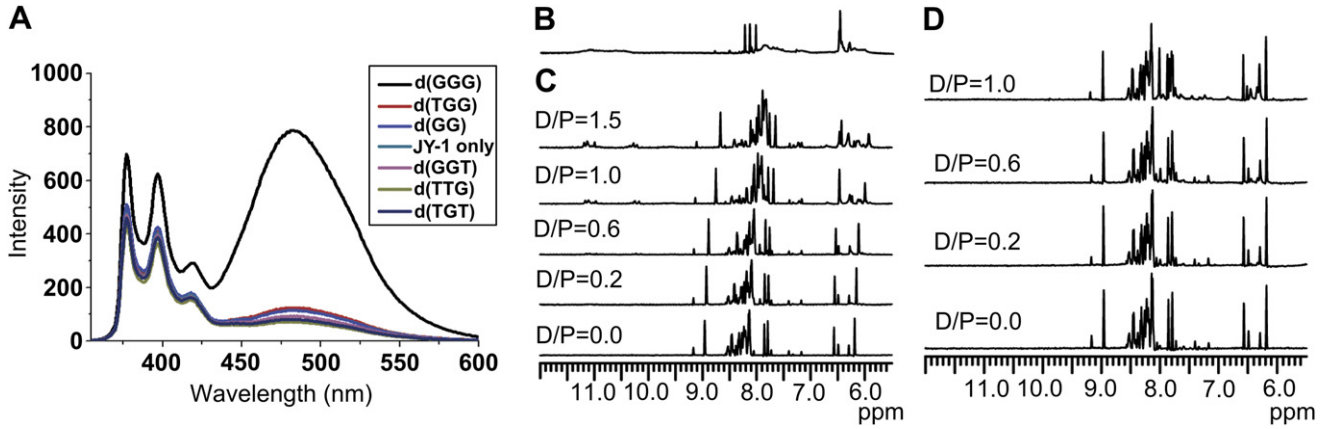

Fig. 3. (A) Fluorescence emission spectra of **JY-1** complexed with DNA trimers (TTG, TGG, GGG, GGT, or GTG) or GG dimer in the aqueous solution containing 10 mM sodium phosphate (pH = 7.0) at D/*P* = 1.0. (B) ^{1}H-NMR spectrum of free GGG in 60% H_2O/10% D_2O/30% CD_3CN buffer containing 5 mM sodium phosphate (pH 8.0) and 50 mM NaCl at 25 °C 1D ^{1}H-NMR spectra of **JY-1** in 60% H_2O/10% D_2O/30% CD_3CN buffer containing 5 mM sodium phosphate (pH 8.0) and 50 mM NaCl at 25 °C upon titration with the (C) GGG or (D) TTG trimers. The D/P ratios are shown on the left of spectra. The part of spectrum in which imino proton region are expaned to emphasize the six imino proton peaks are added on top of Fig. 3C.

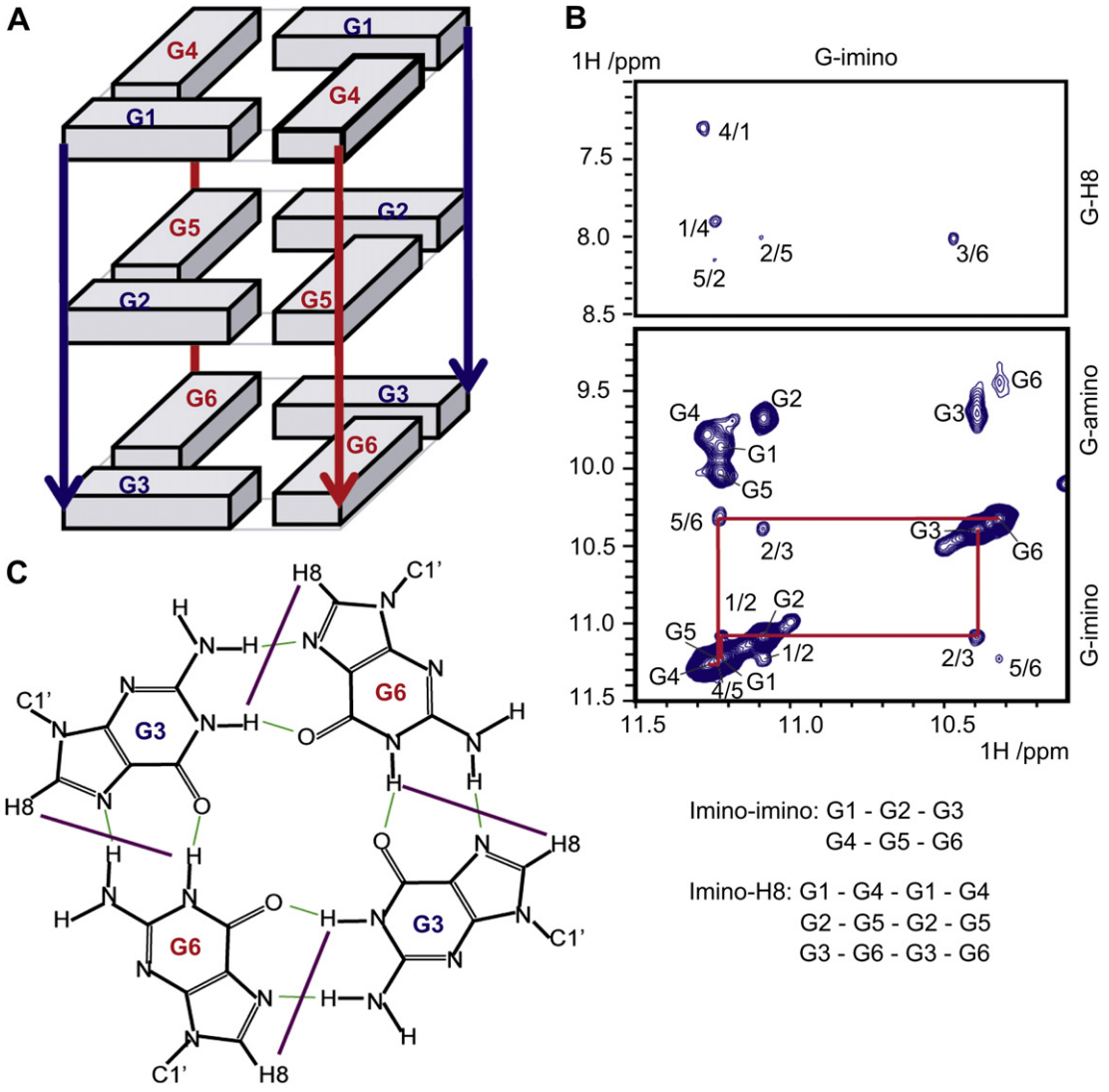

Fig. 4. (A) Schematic structure of tetrameric parallel G-quartet of GGG. (B) Expanded regions (imino-to-base: upper; imino-to-amino: lower) of 2D Watergate NOESY spectra of the **JY-1**–GGG complex (D/P = 1.0) in 60% H_2O/10% D_2O/30% CD_3CN buffer containing 5 mM sodium phosphate (pH 8.0) and 50 mM NaCl at 10 °C. Sequential imino-to-imnio connectivities are represented with red lines. (C) Specific imino-H8 connectivity pattern around a G-tetrad (G•3G6•G3•G6) indicated with magenta lines. (For interpretation of the references to colour in this figure legend, the reader is referred to the web version of this article.)

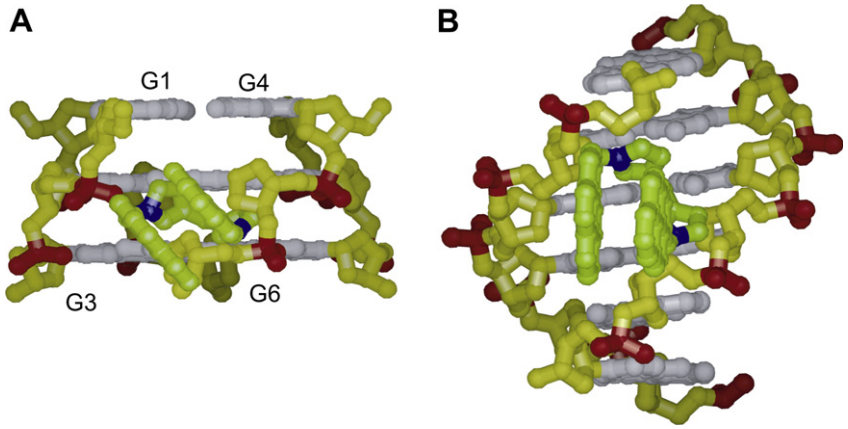

Fig. 5. Representative model for the **JY-1** complexed with (A) parallel G-quartet of GGG and (B) B-form DNA. The **JY-1** atoms are green. Positive charged nitrogen atoms of **JY-1** are blue. The sugar and base atoms of DNA are yellow and white, respectively. Phosphate backbone anions are red. (For interpretation of the references to colour in this figure legend, the reader is referred to the web version of this article.)

intra-residue and sequential NOE connectivities (S-Figure 2). The exchangeable protons were assigned according to their sequential imino-to-imino connectivities and confirmed by intra-residue strong imino-to-amino and weak imino-to-H8 NOE cross peaks in the NOESY spectra (Fig. 4). The chemical shifts of the proton resonances of the GGG in the **JY-1**/GGG complex are given in S-Table 1. The pattern of the imino proton resonances of this complex is very similar to that of the U6 variant of human telomeric sequence, d(TAGGGUTAGGGT), which exhibits dimeric parallel G-quartet structure [38]. The two-fold symmetric parrallel G-quartet structure of GGG satisfied well the sequential imino-to-imino connectivities and unique imino-to-H8 NOE data (Fig. 4). However, none of the models for anti-parrallel G-quartet structures could not explain the NMR NOESY data we observed. Thus, we suggested that **JY-1** is thought to be not just the G-quartet structure-recognizing seonsor but the "G-quartet inducer" which is interacts with the G-rich DNA region and then produces the G-quartet structure.

The main intermolecular interaction in the **JY-1**–DNA complex is electrostatic interaction between the imidazolium moiety of **JY-1** and phosphate anion of DNA. When two imidazolium cations maintain the stacked structure of two pyrene moieties during interaction with DNA, **JY-1** shows the excimer fluorescence. However, when the stacked structure of two pyrene moieties is disrupted to make two imidazolium–DNA interactions, the excimer fluorescence disappears. Fig. 5A shows the possible model structure of the parrallel G-quartet DNA complexed with the **JY-1** that has the stacked two pyrene moieties. Surprisingly, two imidazolium groups could interact with the G1-p-G2 phosphate anion of one strand and with the G5-p-G6 phosphate anion of next strand, respectively (Fig. 5A). However, in the case of normal B-DNA, the phosphate anions across the minor groove cannot maintain the stacked structure of two pyrene moieties through electrostatic interaction with imidazolium groups of **JY-1** (Fig. 5B). This representive model could suggest that **JY-1** binds to GGG sequences on the groove of G-quartet tightly and that this interaction induces excimer emission enhancement of **JY-1**. The binding constant was calculated as $5.5 \times 10^5\ M^{-1}$ (S-Figure 3) and the excimer emission was shown visually in S-Figure 4.

3.5. Circular dichroism and fluorescent change measurement

Circular dichroism (CD) was also used to consider the binding mechanism between **JY-1** and DNAs [39,40]. DNA-3, known as thrombin-binding aptamer, forms the antiparallel G-quadruplex structure in the presence of K^+ ion and exhibits a negative band near 265 nm and a positive band at 290 nm, respectively [41]. As the concentration of **JY-1** increased, there was no appreciable distortion of DNA-3 in the presence of 6 mM KCl, and no induced circular dichroism (ICD) was observed (Fig. 6C). DNA-1 and DNA-2 duplex complexed with **JY-1** showed lowered CD at 280 nm which is related with DNA helix unwinding [42]. We noticed DNA-1 complexed with **JY-1** did not show ICD at the UV absorption range of **JY-1**, but only DNA-2 duplex with **JY-1** showed a weak negative ICD from the pyrene absorption region (Fig. 6A and B). In the presence of DNA duplex, negative ICD band indicates that **JY-1** could destabilize the DNA duplexes. These CD features are consistent with the excimer and monomer emission differences between three DNA duplexes complexed with **JY-1** in the fluorescence study, and no ICD of DNA-3 with **JY-1** supports the groove binding interaction.

To further study the binding mode of **JY-1** with DNA oligonucleotides, we examined the fluorescent changes of **JY-1** with the anionic quencher $Fe(CN)_6^{4-}$. If the binding of **JY-1** involves intercalation to the DNA complex, the fluorescent quenching by $Fe(CN)_6^{4-}$ should be minimally or not effective because the negative charge of the phosphate group creates an electrostatic barrier, so the quencher can't approach the **JY-1** [43]. As shown in S-Figure 5, the anionic quencher $Fe(CN)_6^{4-}$ caused a decrease of excimer emission by **JY-1** complexed with DNA-1 duplex (at $D/P = 0.1$) and this result also confirms that the excimer emission of **JY-1** was induced by the outside binding of DNA complexes.

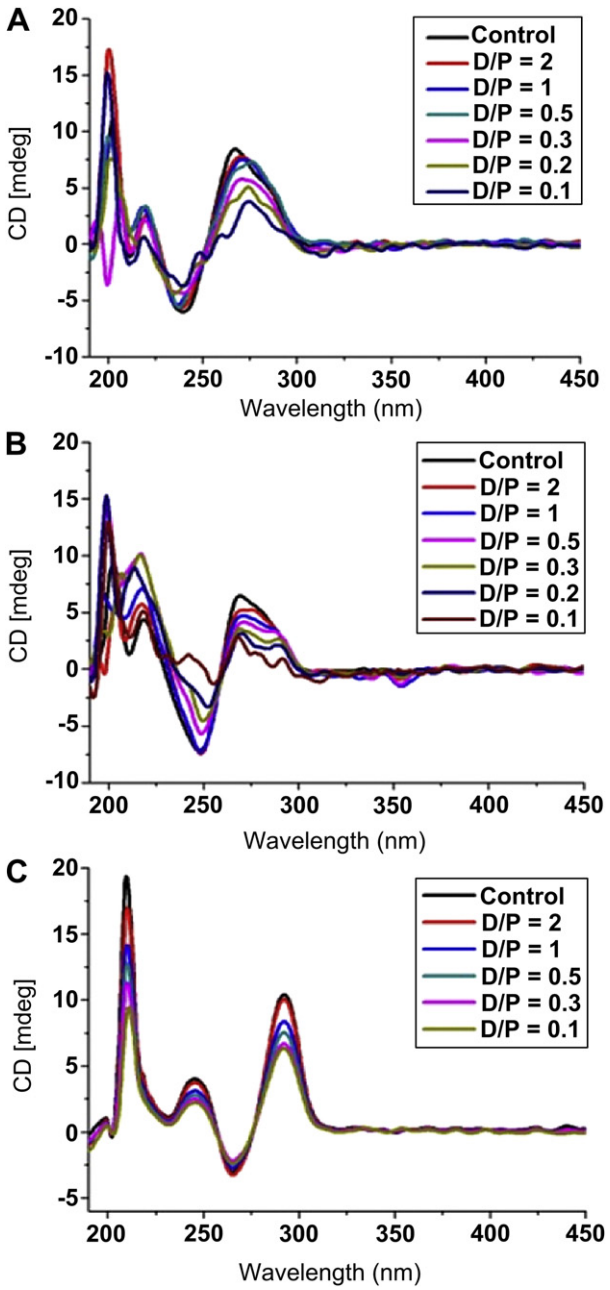

Fig. 6. CD spectra changes of (A) DNA-1 duplex and (B) DNA-2 duplex (6 μM) with various concentration of **JY-1** in 10 mM sodium phosphate buffer (pH 7.0). (C) CD spectra of DNA-3 (6 μM) complexed with various concentration of **JY-1** in HEPES buffer containing 6 mM KCl. DNA/compound **JY-1** ratios ranged from 0.1 to 2 for each titration. (Control : DNA only, D: DNA, P: **JY-1**).

4. Conclusions

We have described a quadruplex selective fluorescent probe, **JY-1**, designed on the structural combination of highly effective binding ability with DNA as well as inducing distinctive fluorescent emission changes. The selectivity of strong binding to a specific

sequence can allow for quadruplex sensing and the detection method presented here is very simple, using fluorescence and NMR study. We found that **JY-1** is thought to be the ''G-quartet inducer'' which is interacts with the G-rich DNA region and then produces the G-quartet structure, contrast to other sensors recognizing the G-quartet DNA structure. Also, the groove binding characteristic of **JY-1** to the G-quadruplex has a relatively low nonspecific toxicity and the structure-specific differences in fluorescent character between DNA duplex and G-quadruplex may offer more discovery and application in biological study.

Acknowledgments

We thank Dr. Jae-Sun Shin and Prof. Byong-Seok Choi for supporting NMR experiments. This work was supported by the NRF Grants (2010-0014199, NRF-C1ABA001-2010-0020480 to J.-H.L.; 2011-0020450, R31-2008-000-10010-0 (WCU) to J.Y.) funded by the Korean Government (MEST). J.-H.L. also thanks to the support by a grant from the Next-Generation BioGreen 21 Program (SSAC, grant #: PJ008109), Rural Development Administration, Republic of Korea. J.Y. also thanks to the support by the Ewha Global Top5 Grant 2011 of Ewha Womans University.

Appendix. Supplementary material

Supplementary data associated with this article can be found, in the online version, at doi:10.1016/j.biomaterials.2011.11.073

References

[1] Kumara GS, Dasa S, Bhadraa K, Maiti M. Protonated forms of poly[d(G-C)] and poly(dG).poly(dC) and their interaction with berberine. Bioorg Med Chem 2003;11(23):4861–70.
[2] Feng X, Liu L, Wang S, Zhu D. Water-soluble fluorescent conjugated polymers and their interactions with biomacromolecules for sensitive biosensors. Chem Soc Rev 2010;39(7):2411–9.
[3] Liu J, Cao Z, Lu Y. Functional nucleic acid sensors. Chem Rev 2009;109(5):1948–98.
[4] Tsui C, Coleman LE, Griffith JL, Bennett EA, Goodson SG, Scott JD, et al. Single nucleotide polymorphisms (SNPs) that map to gaps in the human SNP map. Nucleic Acids Res 2003;31(16):4910–6.
[5] Gomez-Marquez J. DNA G-quadruplex: structure, function and human disease. Febs J 2010;277(17):3451.
[6] Cuesta J, Read MA, Neidle S. The design of G-quadruplex ligands as telomerase inhibitors. Mini Rev Med Chem 2003;3(1):11–21.
[7] Manet I, Manoli F, Zambelli B, Andreano G, Masi A, Cellai L, et al. Affinity of the anthracycline antitumor drugs Doxorubicin and Sabarubicin for human telomeric G-quadruplex structures. Phys Chem Chem Phys 2011;13(2):540–51.
[8] Davis JT. G-quartets 40 years later: from 5'-GMP to molecular biology and supramolecular chemistry. Angew Chem Int Edit 2004;43(6):668–98.
[9] White EW, Tanious F, Ismail MA, Reszka AP, Neidle S, Boykin DW, et al. Structure-specific recognition of quadruplex DNA by organic cations: Influence of shape, substituents and charge. Biophys Chem 2007;126(1–3):140–53.
[10] Song G, Ren J. Recognition and regulation of unique nucleic acid structures by small molecules. Chem Commun 2010;46:7283–94.
[11] He F, Tang Y, Yu M, Feng F, An L, Sun H, et al. Quadruplex-to-duplex transition of G-rich oligonucleotides probed by cationic water-soluble conjugated polyelectrolytes. J Am Chem Soc 2006;128(21):6764–5.
[12] Peng X, Du J, Fan J, Wang J, Wu Y, Zhao J, et al. A selective fluorescent sensor for imaging Cd^{2+} in living cells. J Am Chem Soc 2007;129(6):1500–1.
[13] Zhou Y, Xu Z, Yoon J. Fluorescent and colorimetric chemosensors for detection of nucleotides, FAD and NADH: highlighted research during 2004-2010. Chem Soc Rev 2011;40(5):2222–35.
[14] Kim HN, Guo Z, Zhu W, Yoon J, Tian H. Recent progress on polymer-based fluorescent and colorimetric chemosensors. Chem Soc Rev 2011;40(1):79–93.
[15] Zhang JF, Zhou Y, Yoon J, Kim JS. Recent progress in fluorescent and colorimetric chemosensors for detection of precious metal ions (silver, gold and platinum ions). Chem Soc Rev 2011;40(7):3416–29.
[16] Nagatoishi S, Nojima T, Juskowiak B, Takenaka S. A pyrene-labeled G-quadruplex oligonucleotide as a fluorescent probe for potassium ion detection in biological applications. Angew Chem Int Ed 2005;44(32):5067–70.
[17] Seo YJ, Lee IJ, Yi JW, Kim BH. Probing the stable G-quadruplex transition using quencher-free end-stacking ethynyl pyrene-adenosine. Chem Commun; 2007:2817–9.
[18] Wu Z-S, Hu P, Zhou H, Shen G, Yu R. Fluorescent oligonucleotide probe based on G-quadruplex scaffold for signal-on ultrasensitive protein assay. Biomaterials 2010;31(7):1918–24.
[19] Allain C, Monchaud D, Teulade-Fichou MP. FRET templated by G-quadruplex DNA: a specific ternary interaction using an original pair of donor/acceptor partners. J Am Chem Soc 2006;128(36):11890–3.
[20] Yang P, De Cian A, Teulade-Fichou MP, Mergny JL, Monchaud D. Engineering bisquinolinium/thiazole orange conjugates for fluorescent sensing of G-quadruplex DNA. Angew Chem Int Ed 2009;48(12):2188–91.
[21] Li T, Wang E, Dong S. Parallel G-quadruplex-specific fluorescent probe for monitoring DNA structural changes and label-free detection of potassium ion. Anal Chem 2010;82(18):7576–80.
[22] He F, Tang Y, Wang S, Li Y, Zhu D. Fluorescent amplifying recognition for DNA G-quadruplex folding with a cationic conjugated polymer: A platform for homogeneous potassium detection. J Am Chem Soc 2005;127(35):12343–6.
[23] Zhu J, Li T, Zhang L, Dong S, Wang E. G-quadruplex DNAzyme based molecular catalytic beacon for label-free colorimetric logic gates. Biomaterials 2011;32(30):7318–24.
[24] Paramasivan S, Bolton PH. Mix and measure fluorescence screening for selective quadruplex binders. Nucleic Acids Res 2008;36(17):e106.
[25] Ou TM, Lu YJ, Tan JH, Huang ZS, Wong KY, Gu LQ. G-quadruplexes: targets in anticancer drug design. ChemMedChem. 2008;3(5):690–713.
[26] Xu Z, Kim SK, Yoon J. Revisit to imidazolium receptors for the recognition of anions: highlighted research during 2006-2009. Chem Soc Rev 2010;39(5):1457–66.
[27] Amendola V, Boiocchi M, Colasson B, Fabbrizzi L, Rodriguez Douton M-J, Ugozzoli F. A metal-based trisimidazolium cage that provides six C-H hydrogen-bond-donor fragments and includes anions. Angew Chem Int Ed 2006;45(41):6920–4.
[28] Lu Q-S, Dong L, Zhang J, Li J, Jiang L, Huang Y, et al. Imidazolium-functionalized BINOL as a multifunctional receptor for chromogenic and chiral anion recognition. Org Lett 2009;11(3):669–72.
[29] Kumar S, Luxami V, Kumar A. Chromofluorescent probes for selective detection of fluoride and acetate ions. Org Lett 2008;10(24):5549–52.
[30] Amendola V, Boiocchi M, Colasson B, Fabbrizzi L, Monzani E, Douton-Rodriguez MJ, et al. Redox active cage for the electrochemical sensing of anions. Inorg Chem 2008;47(11):4808–16.
[31] Chen X, Kang S, Kim MJ, Kim J, Kim YS, Kim H, et al. Thin-film formation of imidazolium-based conjugated polydiacetylenes and their application for sensing anionic surfactants. Angew Chem Int Ed 2010;49(8):1422–5.
[32] Xu Z, Singh NJ, Kim SK, Spring DR, Kim KS, Yoon J. Induction-driven stabilization of the anion-pi interaction in electron-rich aromatics as the key to fluoride inclusion in imidazolium-cage receptors. Chem-Eur J 2011;17(4):1163–70.
[33] Chellappan K, Singh NJ, Hwang I-C, Lee JW, Kim KS. A calix[4]imidazolium[2]pyridine as an anion receptor. Angew Chem Int Ed 2005;44(19):2899–903.
[34] Kim HN, Lim J, Lee HN, Ryu JW, Kim MJ, Lee J, et al. Unique x-ray sheet structure of 1,8-bis(imidazolium) anthracene and its application as a fluorescent probe for DNA and DNase. Org Lett 2011;13(6):1314–7.
[35] Kim HN, Moon JH, Kim SK, Kwon JY, Jang YJ, Lee JY, et al. Fluorescent sensing of triphosphate nucleotides via anthracene derivatives. J Org Chem 2011;76(10):3805–11.
[36] Fletcher TMSD, Salazar M, Hurley LH. Effect of DNA secondary structure on human telomerase activity. Biochemistry 1998;37(16):5536–41.
[37] Kan ZY, Yao Y, Wang P, Li XH, Hao YH, Tan Z. Molecular crowding induces telomere G-quadruplex formation under salt-deficient conditions and enhances its competition with duplex formation. Angew Chem Int Ed 2006;45(10):1629–32.
[38] Phan AT, Patel DJ. Two-repeat human telomeric d(TAGGGTTAGGGT) sequence forms interconverting parallel and antiparallel G-quadruplexes in solution: distinct topologies, thermodynamic properties, and folding/unfolding kinetics. J Am Chem Soc 2003 Dec 10;125(49):15021–7.
[39] Lyng R, Hard T, Norden B. Induced CD of DNA intercalators: electric dipole allowed transitions. Biopolymers 1987;26(8):1327–45.
[40] Kim HK, Kim JM, Kim SK, Rodger A, Norden B. Interactions of intercalative and minor groove binding ligands with triplex poly(dA).[poly(dT)]2 and with duplex poly(dA).poly(dT) and poly[d(A-T)]2 studied by CD, LD, and normal absorption. Biochemistry 1996;35(4):1187–94.
[41] Monchaud D, Yang P, Lacroix L, Teulade-Fichou MP, Mergny JL. A metal-mediated conformational switch controls G-quadruplex binding affinity. Angew Chem Int Ed 2008;47(26):4858–61.
[42] Duff MR, Mudhivarthi VK, Kumar CV. Rational design of anthracene-based DNA binders. J Phys Chem B 2009;113(6):1710–21.
[43] Scaria PV, Shafer RH. Binding of ethidium bromide to a DNA triple helix. Evidence for intercalation. J Biol Chem 1991;266(9):5417–23.